# MODELING AND CONTROL OF KEYHOLE ARC WELDING PROCESS

**Y. M. Zhang and Y. C. Liu**

*Welding Research Laboratory*
*Center for Robotics and Manufacturing Systems and*
*Department of Electrical and Computer Engineering*
*College of Engineering, University of Kentucky*
*Lexington, KY 40506, USA*

Abstract: This paper addresses the development of an adaptive control system for keyhole arc welding process. The system developed adjusts the amperage of the peak current to achieve the desired peak current period under varying manufacturing conditions. A nominal model is selected from models identified using experimental data and is used as the *a prior* model of the controlled process. A predictive control algorithm has been designed for the nominal model structure. Closed-loop control experiments have been conducted to verify the effectiveness of the developed system under varying set-point and varying travel speed. *Copyright © 2002 IFAC*

Keywords: Adaptive control, manufacturing, processes, identification, predictive control.

## 1. INTRODUCTION

Keyhole arc welding (KAW), including the keyhole plasma arc welding (PAW) and the keyhole double-sided arc welding being developed at the University of Kentucky (Zhang, *et al*., 2002), has significant advantages over laser welding process in industrial applications in terms of cost, application range, safety, joint preparation etc. However, its weld pool is still larger or wider than that in laser welding. If a control technology can be developed to minimize the heat input and the weld pool, KAW will become an affordable process to applications which otherwise require laser welding.

With normal welding practice using KAW, the keyhole is maintained open. To maintain an open keyhole, the welding current must be sufficient. Because the arc pressure is proportional to the square of the current (Rokhlin and Guu, 1993), the high current blows the melted metal away from the weld pool, causing burn-through. The authors have proposed switching the current from the peak level to a lower base current level after the establishment of the keyhole is detected. In this way, while the establishment of the keyhole ensures the desired full penetration, the melted metal solidifies and the keyhole closes under the base current so that the burn-through is prevented. In this case, the process is not exactly maintained in the keyhole mode of the classical definition, but in a quasi or pulsed keyhole mode.

Although the pulsed keyhole method sounds straightforward, its effectiveness relies on the selection of the peak current. In fact, when the current is switched to the peak level to establish the keyhole, the heat from the arc transfers both radially and axially in the workpiece. If the peak current is high such that the arc pressure is sufficient, the depth of the cavity or the partial keyhole will develop rapidly because the large arc pressure allows the arc to heat deeply underneath the surface. The majority of the heat will transfer axially rather than radially. A deep narrow weld pool, similar as laser weld pool, will form. If the peak current is too low, more heat will be transported radially to generate a shallow wide weld pool. However, if the current is too high, the melted metal may also be detached away from the weld pool before the process responds to the sensor signal. Hence, the selection of the peak current is critical in successfully implementing the pulsed

keyhole process.

Based on analysis above, a double-loop system shown in Fig. 1 is needed to automatically adjust the amperage of the peak current. In the inner loop of the double-loop control system, the pulsation controller switches the current from the peak level to the base level after the keyhole is detected and then switches the current from the base level to the peak level once the base current has been applied for a pre-specified period. In the outer loop, the amperage controller adjusts the amperages of the peak current $(I_p)$ as the control variable to maintain the peak current duration $(T_p)$, which ends when the keyhole is detected, as the output of the system at the desired value which has been pre-specified.

Theoretically, after the system input (control variable) and output are defined, if the output is measurable, the development of the control system becomes a problem of designing a feedback control algorithm based on the dynamic model of the controlled process. However, the dynamic model of the controlled process in general varies with the manufacturing conditions. Hence, it appears that an adaptive control is necessary. In this paper, an adaptive double-loop control system shown in Fig. 1 is proposed and developed.
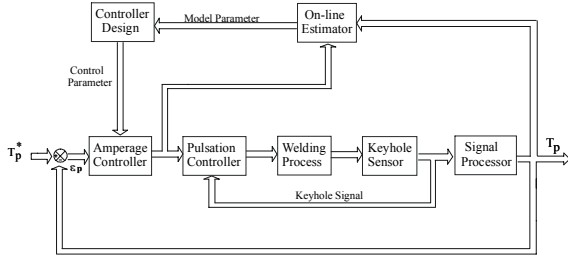


Fig. 1  Adaptive double-loop control system.

## 2.    EXPERIMENTAL SYSTEM

The experimental system includes an arc welding power supply which receives command from an analog interface to adjust its output current, a one-dimensional motion system which receives command from an analog interface to adjust the travel speed, a fixture which holds the workpiece, and a keyhole sensor which provides the information on the state of the keyhole.

## 3.    CONTROLLED PROCESS

It is known, although the start time of the peak current is known and fully controllable, the end time of the peak current is unknown in advance because the current is switched from the peak current to the base current immediately, or a pre-specified delay time, after the keyhole is established and the establishment time of the keyhole is subject to the influence and control of manufacturing conditions and parameters. To ensure the peak current duration $(T_p)$ to reach the desired value $(T_p^*)$, the
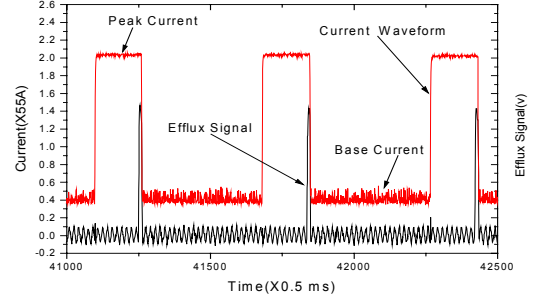


Fig. 2  Typical current waveform and efflux signal during pulsed keyhole plasma arc welding.

amperage of the peak current $(I_p)$ is adjusted as the control variable. Hence, the controlled process is defined by its control variable $I_p$ and output $T_p$.

Fig. 2 shows a typical current waveform and efflux sensor signal recorded during pulsed keyhole arc welding process. At instant $t_1$, the current is switched from the base current to the peak current (Fig. 3). The depths of the weld pool and the partial keyhole then increase under the peak current. At $t_2$, the weld pool becomes fully penetrated and the complete keyhole is established through the thickness of the workpiece. This instant $(t_2)$ can be detected from the efflux signal as the instant when the efflux signal exceeds the pre-set threshold. In Fig. 2, the current is switched from the peak current to the base current right after the establishment of the keyhole is confirmed. In general, the peak current is switched to the base current $d$ seconds $(d \geq 0)$ after the establishment of the keyhole is confirmed. Denote this instant as $t_3$. Then the peak current duration $T_p = t_3 - t_1$. In the case shown in Fig. 2, the delay $d = 0$ and $t_3 = t_2$. Hence, in Fig. 2, $T_p = t_2 - t_1$.

In the proposed pulsed keyhole process, the current is switched back to the peak current $T_b$ seconds after $t_3$ where the base current duration $T_b$ is a pre-programmed fixed parameter. Denote this instant as $t_4$. Assume that the keyhole is confirmed again at $t_5$ and the current is switched to the base current again at $t_6 = t_5 + d$. It is evident that $t_4$ is the $t_1$, $t_5$ is the $t_2$, and $t_6$ is the $t_3$ for the succeeding new pulse cycle. If $t_1$, $t_2$, and $t_3$ are denoted as $t_1(k)$, $t_2(k)$, and $t_3(k)$; $t_3 - t_1$ as $T_p(k)$ and $t_4 - t_3$ as $T_b(k)$; and the peak current between $t_1$ and $t_3$ as $I_p(k)$, and the base current between $t_3$ and $t_4$ as $I_b(k)$. Then $t_4$ is denoted as $t_1(k+1)$, $t_5$ as $t_2(k+1)$, $t_6$ as $t_3(k+1)$; and $T_p(k+1)$, $T_b(k+1)$, $I_p(k+1)$ and $I_b(k+1)$ can be defined accordingly. In this way, the control variable $I_p(k)$ and output $T_p(k)$ sequences which will be used in modeling and control are defined. The dynamic model to be identified is thus a

mathematical relation between the control variable sequence $\{I_p(k)\}$ and the output sequence $\{T_p(k)\}$.

In this study, the controlled process is modeled as a discrete-time time-invariant system by using an autoregressive moving-average (ARMA) difference equation:

$$y(k) - a_1 y(k-1) - \ldots - a_n y(k-n) \\ = b_1 u(k-1) + \ldots + b_m u(k-m) + \eta(k) \quad (1)$$

where $y(k) = T_p(k)$, $u(k) = I_p(k)$, and $\eta(k)$ are the output (peak current duration), the control variable (amplitude of the peak current), and the disturbance at instant $k$ respectively; $a_i (i = 1, \ldots, n)$ and $b_j (j = 1, \ldots, m)$ are the model parameters; $n$ and $m$ are the orders of the autoregressive and moving-average polynomials $A(q^{-1}) = 1 - a_1 q^{-1} - \ldots - a_n q^{-n}$ and $B(q^{-1}) = b_1 q^{-1} + \ldots + b_m q^{-m}$ where $q^{-1}$ is the delay operator. Further, the disturbance is considered a sum of a constant disturbance $c_0$, a moving average of the base current in previous periods $\sum_{l=1}^{o} c_l I_b(k-l)$, and a stochastic process $e(k)$:

$$\eta(k) = c_0 + \sum_{l=1}^{o} c_l I_b(k-l) + e(k) \quad (2)$$

In general, $e(k)$ may be stationary but not white. For simplification, this study assumes the stochastic process be a Gaussian white noise $\varepsilon(k) \sim N(0, \sigma^2)$, i.e., $e(k) = \varepsilon(k)$. As a result, the dynamic model of the controlled process can be expressed as

$$y(k) = c_0 + a_1 y(k-1) + \ldots + a_n y(k-n) + b_1 u(k-1) + \ldots \\ + b_m u(k-m) + c_1 I_b(k-1) + \ldots + c_o I_b(k-o) + \varepsilon(k)$$
(3)

To identify the process, two experiments have been designed and conduced (Liu, 2001). The orders of the identified models are (6,3,1) and (2,2,1). The two model structures identified from the two sets of data are very different. Analysis shows that the time-varying characteristic of the controlled process may have resulted in the higher orders. It is known that during the adaptive control process, the dynamic model of the controlled process will be on-line
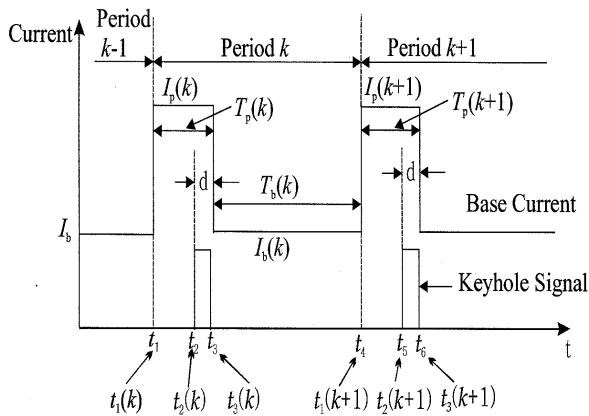


Fig. 3 Dynamic development in pulsed keyhole process.

recursively estimated. Hence, the (2,2,1) is selected as the model structure for control system design. The identified (2,2,1) model will be used as the nominal or the *a prior* model in the control system.

## 4. CONTROL SYSTEM DESIGN

### 4.1 On-line Parameter Identification

Recursive Least Squares algorithm (Ljung, 1997) is used to on-line estimate the parameters. The model of the controlled process can be written as a regression equation:

$$y(k) = \varphi(k)\theta + \varepsilon(k) \quad (4)$$

where

$$\begin{cases} \varphi(k) = (1, y(k-1), y(k-2), u(k-1), u(k-2), I_b(k-1))^T \\ \theta = (c_0, a_1, a_2, b_1, b_2, c_1)^T \end{cases} \quad (5)$$

The recursive equations are

$$\begin{cases} \hat{\theta}(k) = \hat{\theta}(k-1) + K(k)(y(k) - \varphi^T(k)\hat{\theta}(k-1)) \\ K(k) = P(k)\varphi(k) = \dfrac{P(k-1)\varphi(k)}{(\lambda + \varphi^T(k)P(k-1)\varphi(k))} \\ P(k) = \dfrac{1}{\lambda}(I - K(k)\varphi^T(k))P(k-1) \end{cases} \quad (6)$$

where $\gamma$ is forgetting factor, and

$$\hat{\theta}(k) = (\hat{c}_0(k), \hat{a}_1(k), \hat{a}_2(k), \hat{b}_1(k), \hat{b}_2(k), \hat{c}_1(k))^T \quad (7)$$

is the estimate of the parameter vector at instant $k$.

### 4.2 GPC Algorithm

The generalized predictive control (GPC) (Clarke, *et al.*, 1987) is capable of controlling plants with variable parameters, variable dead-time, and variable orders. This algorithm is used in this study to control the underlying process described by

$$y(k) = c_0 + a_1 y(k-1) + a_2 y(k-2) + \\ + b_1 u(k-1) + b_2 u(k-2) + c_1 I_b(k-1) + \varepsilon(k) \quad (8)$$

For a specific application, the base current is fixed at a predetermined value and remains constant during control. Denote $\tilde{c}_0 = c_0 + c_1 I_b$. Then $\tilde{c}_0$ can be considered as a constant and can be determined using the nominal values of $(c_0, c_1)$, as identified from the off-line experiments or directly on-line identified. Hence, the model reduces to

$$A(q^{-1})y(k) = \tilde{c}_0 + b_1 u(k-1) + b_2 u(k-2) + \varepsilon(k) \quad (9)$$

where $q^{-1}$ is the back-shift operator, and $A(q^{-1}) = 1 - a_1 q^{-1} - a_2 q^{-2}$.

Consider the following Diophantine equation:

$$A E_j + q^{-j} F_j = 1 \quad (10)$$

where $\deg(E_j) = j - 1, \deg(F_j) = 1$, and

$$E_j = 1 + e_1 q^{-1} + \ldots + e_{j-1} q^{-(j-1)} \quad (11)$$

$$F_j = f_{j,0} + f_{j,1} q^{-1} \quad (12)$$

To solve for equation (10), combining (10) with

$$A E_{j+1} + q^{-(j+1)} F_{j+1} = 1 \quad (13)$$

produces

$$(1 - a_1 q^{-1} - a_2 q^{-2})q^{-j}e_j +$$
$$+ q^{-(j+1)}(f_{j+1,0} + f_{j+1,1}q^{-1}) - q^{-j}(f_{j,0} + f_{j,1}q^{-1}) = 0 \quad (14)$$

Then,

$$e_j = f_{j,0} \quad (15)$$

$$f_{j+1,1} = a_2 f_{j,0} \quad (16)$$

$$f_{j+1,0} = f_{j,1} + a_1 f_{j,0} \quad (17)$$

When $j = 1$,

$$(1 - a_1 q^{-1} - a_2 q^{-2}) + (f_{1,0}q^{-1} + f_{1,1}q^{-1}) = 0 \quad (18)$$

$$f_{1,0} = a_1 \quad (19)$$

$$f_{1,1} = a_2 \quad (20)$$

Hence, the Diophantine equation (10) can be solved for $E_j$ and $F_j$ recursively using equations (15) ~ (20).

Multiple $E_j$ on both sides of Eq. (8) and then combine with Eq. (9). As a result,

$$y(k + j) = F_j y(k) +$$
$$+ [\widetilde{c}_0 + b_1 u(k + j - 1) + b_2 u(k + j - 2)]E_j + E_j \varepsilon(k + j) \quad (21)$$

$y(k + j)$ is considered as a $j$-step-ahead prediction made at the present instant $k$. Because the prediction to the future white noise is its mean, i.e., 0, the following prediction equation is obtained:

$$\hat{y}(k + j) = (f_{j,0} + f_{j,1}q^{-1})y(k) +$$
$$+ E_j[\widetilde{c}_0 + b_1 u(k + j - 1) + b_2 u(k + j - 2)] \quad (22)$$

Consequently,

$$\begin{cases} y(k+1) = (f_{1,0} + f_{1,1}q^{-1})y(k) + [\widetilde{c}_0 + b_1 u(k) + b_2 u(k-1)] \\ y(k+2) = (f_{2,0} + f_{2,1}q^{-1})y(k) + \\ \qquad + (1 + e_1 q^{-1})[\widetilde{c}_0 + b_1 u(k+1) + b_2 u(k)] \\ \cdots\cdots\cdots \\ y(k+j) = (f_{j,0} + f_{j,1}q^{-1})y(k) + (1 + e_1 q^{-1} + \ldots \\ \qquad + e_{j-1}q^{-(j-1)})[\widetilde{c}_0 + b_1 u(k+j-1) + b_2 u(k+j-2)] \end{cases} \quad (23)$$

Denote
$$\hat{Y} = (\hat{y}(k + 1), \hat{y}(k + 2), \ldots, \hat{y}(k + j))^T$$

$$\Gamma_j = \begin{bmatrix} f_{1,0} & f_{1,1} \\ f_{2,0} & f_{2,1} \\ \cdots\cdots \\ f_{j,0} & f_{j,1} \end{bmatrix}, Y_p = [y(k), y(k-1)]^T,$$

$$\Xi_j = \begin{bmatrix} 1 & 0 & 0 \\ 1 & e_1 \ldots 0 \\ \cdots\cdots \\ 1 & e_1 \ldots e_{j-1} \end{bmatrix}, \Xi_{j-1} = \begin{bmatrix} 1 & 0 & 0 \\ 1 & 0 & 0 \\ 1 & e_1 \ldots 0 \\ \cdots\cdots \\ 1 & e_1 \ldots e_{j-2} \end{bmatrix},$$

$$\widetilde{E} = [1, e_1, \ldots, e_{j-1}]^T$$
and
$$I_j = [1, \ldots, 1]^T_{1 \times j}, I_{j-1} = [1, \ldots, 1]^T_{1 \times (j-1)};$$

the dimensions of $I_j$ and $I_{j-1}$ are $1 \times j$ and $1 \times (j-1)$ respectively. Then,

$$Y = \Gamma Y_p + \widetilde{c}_0 \Xi_j I_j + b_1 \Xi_j I_j u(k + 1) +$$
$$+ b_2 \Xi_{j-1} I_{j-1} u(k + 1) + b_2 \widetilde{E} u(k) \quad (24)$$

Suppose $y_0(k + i)$ is the sequence of the set-point of the output and $y_s(k + i)$ is the smoothed reference sequence and is obtained from a simple first-order lag model with a smoothing factor $\alpha$:

$$y_s(k + i) = \alpha y_s(k + i - 1) + (1 - \alpha)y_0(k + i) \quad (25)$$

with the following initial

$$y_s(k) = y(k) \quad (26)$$

where $y(k)$ is the feedback of the output. A slower transition will be achieved, but with a better robustness if a larger $\alpha$ is used; otherwise, if a smaller $\alpha$ is used, a faster transition can be obtained but with a poorer robustness. Hence, the appropriate value of $\alpha$ depends directly on the model accuracy.

Consider the following cost function:

$$J = E\{\sum_{i=1}^{N_t}[(y(k+i) - y_s(k+i))^2 + \lambda(u(k+i) - I_c)^2]\}$$
$$= \sum_{i=1}^{N_t}[(y(k+i) - y_s(k+i))^2 + \lambda(u(k+i-1) - I_c)^2]$$
$$= \sum_{i=1}^{N_t}[(y(k+i) - y_s(k+i))^2] + \lambda(U - I_{iden})^T(U - I_{iden}) \quad (27)$$

where $I_{iden} = [I_c, I_c, \ldots, I_c]^T_{N_t \times 1}$ is a $N_t \times 1$ vector and $U = [u(k), u(k+1), \ldots, u(k + N_t - 1)]^T$ is the control vector consisting of the current and future control actions, $N_t$ is the prediction horizon which is the maximum step of the predictions and needs to be determined based on the nominal open-loop response, $\lambda$ is the weighting coefficient of the penalty on the deviation of the control action (peak current) from a specified current value $I_c$. In this study, $N_t = 10$ is selected.

The control law is

$$U : \min_U J \quad (28)$$

In the GPC theory, there is a key assumption that is beneficial in improving the system robustness and simplifying the calculation. The assumption is that there exists a "control horizon" beyond which all control changes are zero (Clarke, *et al.*, 1987). We need to determine a positive integer $N_u \le N_t$ as the control horizon which can be considered as the number of the free control actions including the current control action $u(k)$ and future control actions $u(k+1), u(k+2), \ldots, \cdot u(k + N_u - 1)$.

Assume

$$u(k) = u(k+1) = \ldots = u(k + N_t - 1) \quad (29)$$

In this case, $N_u = 1$ is selected as in other applications (Montague, *et al.*, 1986; Zhang, *et al.*, 1996). The solution of the control law is

$$u(k) = \frac{\lambda N_t I_c - (\Gamma Y + \Xi_j I_j \widetilde{c}_0 + b_2 \Xi_2 u(k-1) - Y_s)^T \Delta}{\lambda N_t + \Delta^T \Delta} \quad (30)$$

where

$$\Delta = b_1 \Xi_j I_j + b_2 \Xi_{j-1} I_{j-1} \qquad (31)$$

$$Y_s = [y_s(k+1),...,y_s(k+N_t-1)]^T \qquad (32)$$

Eq. (30) is the designed predictive control algorithm for the outer loop of the double-loop control system.

Simulations suggest that 0.7, 0.9, and 0.95 are acceptable values for $\alpha$, $\lambda$, and $\gamma$, respectively. Using these parameters, no significant steady-state errors are observed and the regulation speed is acceptable. Hence, those parameters and the forgetting factor will be used in the GPC algorithm and the recursive identification algorithm for control experiments.

## 5. CONTROL EXPERIMENTS

The developed control algorithm has been used to conduct closed-loop control experiments under variable set-point and variable travel speed. The material used in experiments is stainless steel (type 304). The thickness of the plate is 3.2 mm and the dimensions of the workpiece are 250 mm in length and 50 mm in width. The sampling period is the pulse cycle which consists of the fixed base current duration 420 mm and the variable peak current duration. Pure argon is used as the shielding gas and the orifice gas.

In all closed-loop control experiments, a pre-designed random sequence is applied as the input during the beginning period. The duration of the beginning period varies from experiment to experiment in the range from 35 to 40 weld cycles. During this period, the parameters are estimated using the nominal model's parameters as the initials. However, the on-line estimated parameters are not actually used in the control until this beginning period ends. The travel speed is 2 mm/s for all experiments except for the varying travel speed experiment.

### 5.1 Open-loop Experiment
Before the closed-loop control experiments are conducted, an open-loop experiment has been done with a constant input $I_p = 115A$. It is observed that despite the constant input peak current, the resultant output peak current period fluctuates in addition to a shift with the time (Liu, 2001). This suggests that the controlled process is subject to an inherent disturbance.

Analysis shows that this disturbance is not caused by any external sources. Instead, it is a type of nature of the controlled process. In fact, as shown in a previous study (Zhang and Ma, 2002), when the keyhole is being established, the process is in an instable state. It is believed that during this instable period, the geometry of the partial (non-penetrated) keyhole experiences a strong fluctuation as determined by the balance between the surface tension, the plasma pressure, and the hydrostatic pressure before the keyhole is finally established. The establishment of the keyhole is thus subject to certain stochastic vibration or fluctuation. This inherent vibration or fluctuation places a difficulty for the control of the keyhole arc welding process.

### 5.2 Varied Set-point
Varied set point is designed to verify the response speed of the GPC control system. The step set-point change is applied from 210 ms to 150 ms at the 100th weld cycle. The resultant output and control variable are plotted in Fig. 4 (a) and (b), respectively. As can be seen, the output $T_p$ can track the set-point change with an acceptable speed and accuracy. The response speed and accuracy are similar as those in the simulation.

Of course, fluctuations are observed in the output in Fig. 4. However, these fluctuations in the output are similar as those in the open-loop experiment and are caused by the inherent disturbances of the controlled process. It appears that the inherent disturbance of the controlled process has not produced significant influence on system's performance.

### 5.3 Varying Travel Speed
The travel speed and the welding current are the two most important welding parameters determining the heat input into the workpiece (Zhang and Kovacevic, 1998). In this experiment, the travel speed changes from 2.18 mm/s to 2.47 mm/s at the 69th cycle, then from 2.47 mm/s to 3.2mms/ at the 138th cycle, then back to 2.47 mm/s at the 142th cycle, and finally to 2.73 mm/s at the 154th cycle. Because of the large change in the speed, large disturbances are suddenly applied.

The output and control action after the speed increase at 69th cycle can be seen in Fig. 5. It is known that an increase in the travel speed will cause a longer time for a given peak current to establish the keyhole. Hence, in order to maintain the output, i.e., the peak
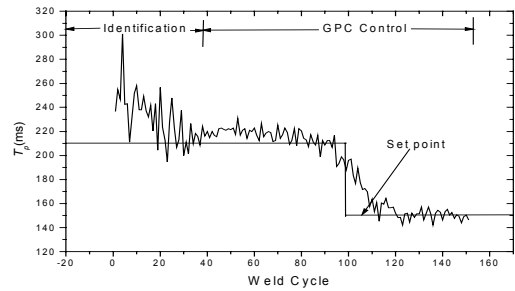


(a) Output
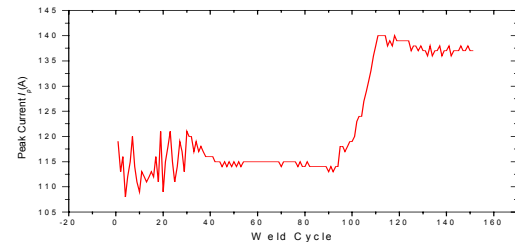


(b) Control action

Fig. 4 Experiment under set-point step change

current period at the desired set-point, the peak current should increase. As can be seen in Fig. 5(b), after the speed is increased at $t = 69$ cycle, the peak current keeps increasing. As a result, the influence of the travel speed increase on the output is naturalized. Of course, because of the large increase in the travel speed, the parameters in the model greatly changed. This sudden change in the model parameters is expected to largely affect the dynamic behaviors of the closed-loop control system. However, as can be seen in Fig. 5, except for a large impact on the control action right after the travel speed is changed at the $69^{th}$ cycle, the control action responds smoothly.

Between $t = 138$ to $t = 154$, the speed is first increased to 3.2 mm/s from 2.47 mm/s at $t = 138$, then changed back to 2.47 mm/s at $t = 142$, and finally increased to 2.73 mm/s at $t = 154$. In this case, large speed impacts and changes are applied. These impacts and increases caused large fluctuations in the control action. However, the output only briefly fluctuated below the set-point. It appears that the system quickly "realized" its "over-reaction" and rapidly corrected the "mistake". As a result, after a brief period of fluctuations, the control action became smooth again. Of course, the fluctuations in the control action were actually caused by the sudden changes in the model parameters. Because of the large fluctuations in the control action and the resultant fluctuations in the output, the estimates of the parameters quickly converged to the new values so that the model and

the control action became accurate and smooth respectively again.

## 6. CONCLUSIONS

Open-loop experiment showed that the controlled process possesses an inherent stochastic disturbance. Although this inherent stochastic disturbance is uncontrollable, the closed-loop control system should not be affected by this disturbance. It was found that the effect of this disturbance in the closed-loop control response was insufficient. Closed-loop control experiments under step set-point change and large travel speed changes and impacts verified the effectiveness of the developed control system.

## ACKNOWLEDGEMENT

## REFERENCES

Clarke, D.W., C. Mohtadi, and P.S. Tuffs (1987). "Generalized predictive control—Part 1", *Automatica*, **Vol. 23**, pp. 137-148,1987.

Liu, Y.C. (2001). Adaptive Control of Plasma Arc Welding Process, *MSEE Thesis*, University of Kentucky, September.

Ljung, L., (1997). System Identification-Theory for the user, $2^{nd}$ Edition, Prentice Hall, Upper Saddle River, NJ.

Montague, G. A., et al. (1986). "On-line estimation and adaptive control of penicillin fermentation," *IEE Proceedings D: Control Theory and Applications*, **Vol. 33**, pp. 240-246.

Rokhlin, S. I. and A. C. Guu (1993). "A study of arc force, pool depression, and weld penetration during gas tungsten arc welding," *Welding Journal*, **72(8):** 381s-390s.

Zhang, Y. M., R. Kovacevic, and L. Li, (1996). "Adaptive control of full penetration GTA welding," *IEEE Transactions on Control Systems Technology*, **4(4):** 394-403.

Zhang, Y. M. and R. Kovacevic (1998). "Neurofuzzy model based control of weld fusion zone geometry," *IEEE Transactions on Fuzzy Systems*, **6(3):** 389-401.

Zhang, Y. M. and Y. Ma (2001) "Stochastic modeling of plasma reflection during keyhole arc welding," *Measurement Science and Technology,* **12(11):** 1964-1975.

Zhang, Y.M., S. B. Zhang and M. Jiang, (2002). "Sensing and control of double-sided arc welding process," to appear in the *ASME Journal of Manufacturing Science and Engineering*.
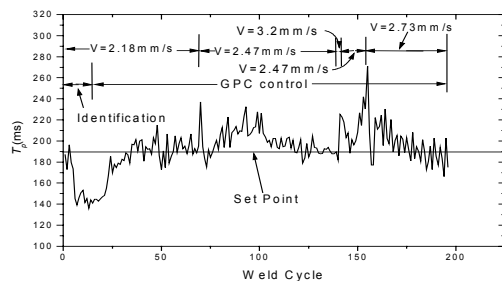
(a) Output
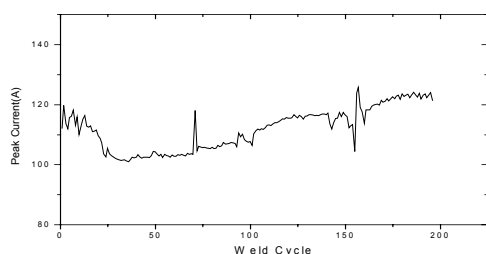


(b) Control action

Fig. 5 Experiment under varying travel speed.